Poliovirus infection blocks ERGIC-to-Golgi trafficking and induces microtubule-dependent disruption of the Golgi complex

Oren Beske[1,*], Mike Reichelt[2,*], Matthew P. Taylor[2], Karla Kirkegaard[2] and Raul Andino[1,‡]

[1]Department of Microbiology and Immunology, University of California, San Francisco, San Francisco, CA 94143, USA
[2]Department of Microbiology and Immunology, Stanford University School of Medicine, Stanford, CA 94305, USA
*These authors contributed equally to this work
‡Author for correspondence (e-mail: Raul.Andino@ucsf.edu)

Accepted 5 July 2007
Journal of Cell Science 120, 3207-3218 Published by The Company of Biologists 2007
doi:10.1242/jcs.03483

Summary

Cells infected with poliovirus exhibit a rapid inhibition of protein secretion and disruption of the Golgi complex. Neither the precise step at which the virus inhibits protein secretion nor the fate of the Golgi complex during infection has been determined. We find that transport-vesicle exit from the endoplasmic reticulum (ER) and trafficking to the ER-Golgi intermediate compartment (ERGIC) are unaffected in the poliovirus-infected cell. By contrast, poliovirus infection blocks transport from the ERGIC to the Golgi complex. Poliovirus infection also induces fragmentation of the Golgi complex resulting in diffuse distribution of both large and small vesicles throughout the cell. Pre-treatment with nocodazole prevents complete fragmentation, indicating that microtubules are required for poliovirus-induced Golgi dispersion. However, virally induced inhibition of the secretory pathway is not affected by nocodazole, and Golgi dispersion was found to occur during infection with mutant viruses with reduce ability to inhibit protein secretion. We conclude that the dispersion of the Golgi complex is not in itself the cause of inhibition of traffic between the ERGIC and the Golgi. Instead, these phenomena are independent effects of poliovirus infection on the host secretory complex.

Supplementary material available online at
http://jcs.biologists.org/cgi/content/full/120/18/3207/DC1

Key words: Virus-cell interaction, Protein secretion, RNA replication

Introduction

The study of how viruses interfere with cellular processes has led to an understanding of many aspects of normal cell function including gene expression (Farabaugh, 1996; Flint and Shenk, 1997; Moss et al., 1991; Mountford and Smith, 1995), cell cycle regulation (Messerschmitt et al., 1997; Moran, 1993), protein secretion (Balch et al., 1994; Dascher et al., 1994; Kuge et al., 1994; Nuoffer et al., 1994; Pind et al., 1994; Presley et al., 1997; Scales et al., 1997), and nuclear import and export (Nakielny and Dreyfuss, 1999; Yoneda et al., 1999). Cells infected with poliovirus display a number of phenotypic alterations collectively called the cytopathic effect. Among these alterations are inhibition of transcription by RNA polymerase II (Clark et al., 1993; Crawford et al., 1981; Kliewer and Dasgupta, 1988), inhibition of translation in host cells (Ehrenfeld, 1982; Helentjaris and Ehrenfeld, 1977; Jen et al., 1978; Jen et al., 1980) and the inhibition of protein secretion (Doedens and Kirkegaard, 1995).

Poliovirus is a positive-stranded RNA virus that replicates its genome in tight association with virus-induced cytoplasmic vesicles (Bienz et al., 1987; Bienz et al., 1992; Caliguiri and Tamm, 1970). Translation of the poliovirus genome results in a single 220 kDa protein that is autoproteolytically processed to yield 11 individual proteins. Most of the non-structural poliovirus proteins, including 2B, 2C, 2BC, 3A and 3CD, associate with the viral-induced vesicles. Notably, all these proteins are produced in the cytoplasm and appear to lack lipid modification. It is thought that 2BC and 3A associate with membranes through hydrophobic domains. The N-terminal region of 2C is predicted to fold into an amphipathic α-helix that is responsible for the association of the protein with membranes in the viral RNA replication complex (Teterina et al., 1997; Teterina et al., 2006). Protein 3A employs a C-terminal hydrophobic domain that confers all the biophysical properties expected in an integral membrane protein (Wessels et al., 2006). Proteins 2BC and 3A have also been shown to exert potent effects on intracellular membranes when expressed individually in cells (Cho et al., 1994; Barco and Carrasco, 1995; Doedens et al., 1997; Suhy et al., 2000). For example, the expression of poliovirus 3A protein inhibits protein secretion and colocalizes with ER markers (Doedens and Kirkegaard, 1995). The overexpression of 2B protein has led to conflicting conclusions. One report showed that 2B inhibits secretion and colocalizes with a seemingly intact Golgi complex (Doedens and Kirkegaard, 1995). However, a different study found that expression of protein 2B results in a disruption of the Golgi complex (Sandoval and Carrasco, 1997). Expression of protein 2C results in massive membrane alterations and disruption of Golgi stacks (Cho et al., 1994), although this causes no apparent disruption of protein secretion (Doedens and Kirkegaard, 1995).

An important consideration regarding these studies with

individual proteins is that the morphological membrane alterations seen in poliovirus-infected cells are not phenocopied by the expression of any single poliovirus protein. This may indicate that the viral program for the remodeling of the secretory complex requires the concerted action of multiple viral proteins and other viral structures. In fact, more recently, it has been shown that the co-expression of poliovirus proteins 2BC and 3A results in an intracellular morphology, and an association of cellular markers that more closely resembles that of the infected cell (Jackson et al., 2005; Suhy et al., 2000). Thus, to gain further insight into the physiological mechanism of poliovirus-induced inhibition of secretion, it is important to analyze these phenomena as they occur in the context of the infected cell.

Here, we have used confocal fluorescence microscopy to examine secreted cargo and Golgi complex during poliovirus infection. Our results show that poliovirus infection has two major consequences for the secretory complex. First, the previously observed block in the ER-to-Golgi traffic occurs at the level of targeting or fusion of post-ERGIC transport vesicles with the Golgi network. Second, as previously described (Sandoval and Carrasco, 1997), poliovirus infection induces a dramatic disruption of the Golgi complex. Early during infection, we observed a loss of the cohesive Golgi structure accompanied by a dispersion of the organelle throughout the cytoplasm. Here, we find that this dispersion of Golgi elements by poliovirus is abrogated by nocodazole whereas protein secretion remains inhibited. Furthermore, Golgi disruption was observed during infection by a poliovirus mutant that displays greatly reduced inhibition of protein secretion. These data suggest that poliovirus induces an inhibition of protein secretion that can be uncoupled from dispersion of the Golgi complex.

Results

Secreted protein cargo accumulates in the ER-to-Golgi intermediate compartment during poliovirus infection

Upon infection with poliovirus, ER-to-Golgi traffic is known to be disrupted, although the precise step, between the ER and the medial Golgi (where Endo H resistance is acquired), at which this disruption occurs has not been identified (Doedens et al., 1997). As shown by immunofluorescence microscopy, the secretory cargo in poliovirus-infected cells is retained in diffuse structures that were found to colocalize with the ER marker calnexin (Doedens et al., 1997). To determine the precise step at which poliovirus disrupts vesicle trafficking and protein secretion, we examined the integrity and function of early secretory compartments using a temperature-sensitive variant of vesicular stomatitis virus G (VSVG), variant VSVG-ts045-GFP, expressed as a fusion protein with GFP (Hirschberg and Lippincott-Schwartz, 1999). Like most membrane proteins, VSVG is co-translationally translocated into the ER and, within minutes, exits the ER and transits sequentially through the ERGIC and Golgi (Hirschberg et al., 1998). At 40°C, however, the VSVG temperature-sensitive allele is retained and accumulates in ER-like structures (Fig. 1A). Upon downshifting to the permissive temperature, VSVG-ts045-GFP is released from the ER to localize in ERGIC and Golgi (Fig. 1A). We thus examined the fate of VSVG-ts045-GFP in poliovirus-infected cells upon release from retention in the ER. In contrast to the results in uninfected cells (Fig. 1A), little Golgi-like VSVG staining was be observed in infected cells after 30 minutes of incubation at the permissive temperature (Fig. 1B). Instead, the VSVG-ts045-GFP was found in both diffuse, ER-type membranes and bright punctate structures (Fig. 1B).

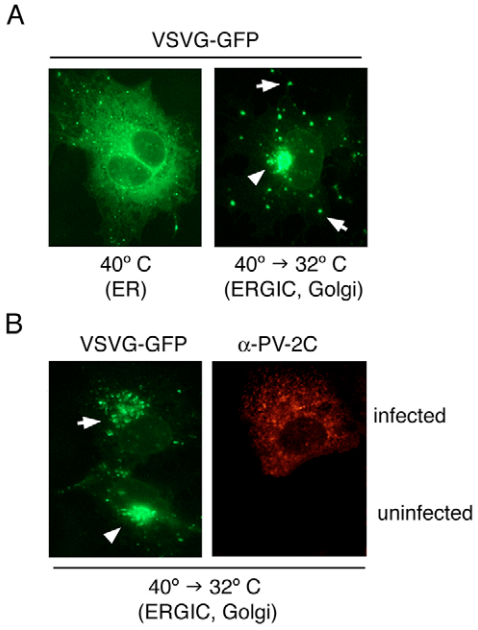

Fig. 1. Transport of VSVG-ts045-GFP protein during poliovirus infection. HeLa cells were transfected with VSVG-ts045-GFP-expressing plasmid and incubated at 40°C overnight to accumulate VSVG-ts045-GFP protein in the ER. (A) Uninfected HeLa cells were either maintained at 40°C (A, left image) or shifted to 32°C for 30 minutes as indicated. The cells were subsequently fixed and mounted for fluorescence microscopy. (B) VSVG-ts045-GFP transfected cells were infected with poliovirus at an MOI of 0.5 PFU/cell at 40°C for 3.5 hours then shifted to 32°C for 30 minutes Cells were then fixed and analyzed for GFP fluorescence or the presence of poliovirus 2C protein by indirect immunofluorescence as indicated to distinguish between uninfected cells and infected cells in the same image. Arrowheads indicate Golgi complexes, arrows indicate ERGIC puncta.

The distinct behavior of VSVG-ts045-GFP in infected versus uninfected cells was further examined in Huh7 cells (Fig. 2). We employed Huh7 cells because their flattened morphology in adherent culture is better suited to confocal microscopy. In uninfected cells, VSVG-ts045-GFP was found to transit from a diffuse ER staining to a juxtanuclear Golgi structure via bright puncta likely to represent the ER-to-Golgi intermediate (ERGIC) compartment (Fig. 2A). Quantitation of cells containing puncta (Fig. 2C) supported the notion that these ERGIC-like puncta are intermediate structures moving from the ER to the Golgi. While in poliovirus-infected cells, the diffuse ER-specific staining gave way to punctate staining patterns at the same rates as in uninfected cells (Fig. 2C), most infected cells retained their punctate staining pattern, even 20 minutes after temperature shift (Fig. 2B,C).

We next determined the identity of the punctate, VSVG-ts045-GFP-containing structures in poliovirus-infected cells. We hypothesized that they represent ERGIC, but could also arise from aberrantly vesiculated Golgi or ER membranes.

However, we observed substantial levels of colocalization between VSVG-ts045-GFP cargo and the ERGIC resident ERGICp53 (Hauri et al., 2000) at both 20 minutes and 60 minutes after a shift to 32°C (Fig. 3). Notably, VSVG-ts045-GFP colocalized with the ERGIC marker in the punctate structures, whereas part of VSVG-ts045-GFP remained as ER-like diffuse staining. We thus infer that a significant portion of the secretory cargo in poliovirus-infected cells escapes the ER and is transported as far as the ERGIC, whereas some remained in ER-like membranes, possibly owing to saturation of the ERGIC.

To visualize the cargo-containing structures that accumulate during poliovirus infection in more detail, we performed electron microscopy (EM) of uninfected and infected cells expressing secreted alkaline phosphatase (SEAP). SEAP is a secretory cargo whose phosphatase activity can be detected histochemically (Mayahara et al., 1967; Yamamoto et al., 2003). Both uninfected (Fig. 4A) and infected (Fig. 4B-D) cells contained SEAP-positive vesicles of approximately 100 nm in diameter. As judged by their morphology, the presence of secretory cargo and their proximity to structures characteristic of both ER and ERGIC, these 100-nm vesicles are likely to be COPII vesicles, which bud from the ER en route to the ERGIC. As previously reported (Suhy et al., 2000), infected cells contained larger (200-400 nm) double-membraned vesicles that accumulated during poliovirus infection, but did not contain SEAP activity in the interior lumen (Fig. 4C). In addition, SEAP-containing structures whose size and morphology are consistent with that of the ERGIC were also observed in poliovirus-infected cells (Fig. 4D). The presence of cargo in these ERGIC structures was confirmed by double staining for SEAP and immunogold labeling of the ERGICp53 marker (Fig. 4E).

These results are consistent with the hypothesis that traffic from the ER to the ERGIC is not directly inhibited during poliovirus infection. Instead, it appears that poliovirus infection blocks the secretory pathway by targeting progression from ERGIC to Golgi, without affecting the budding of COPII vesicles from the ER or delivery of their cargo to the ERGIC.

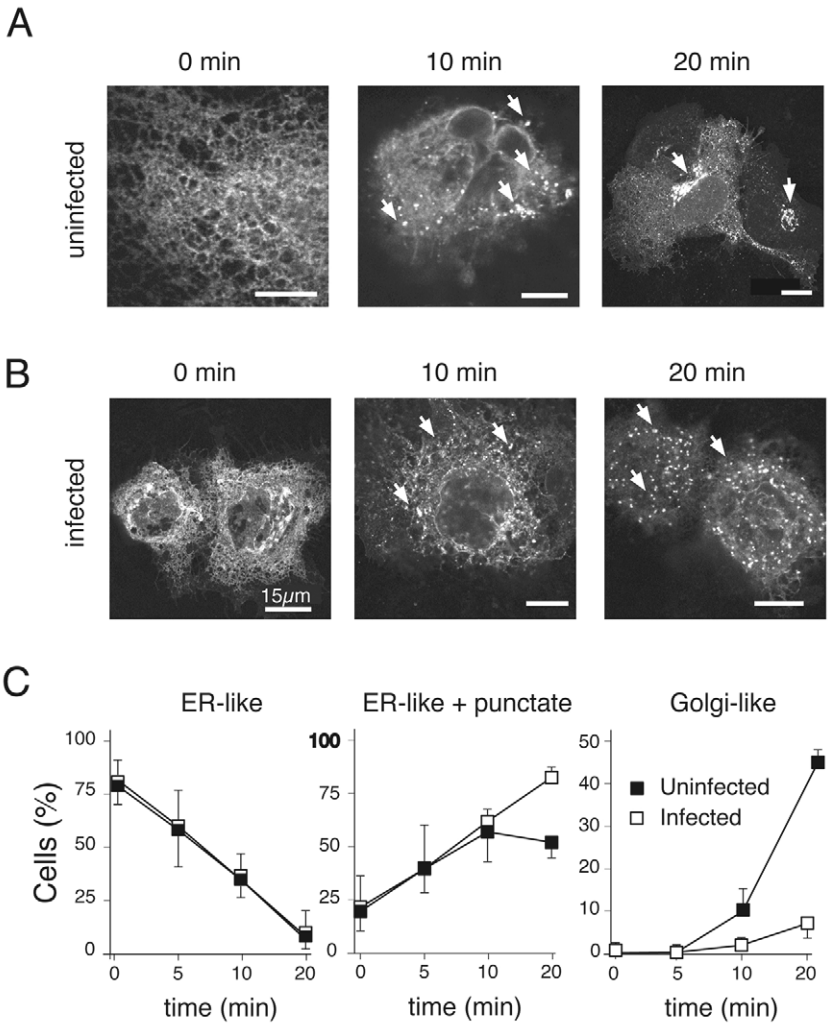

Fig. 2. Confocal microscopy of VSVG-ts045-GFP protein transport during poliovirus infection. Huh7 cells were transiently transfected with VSVG-ts045-GFP for 16 hours at 40°C. (A) Uninfected cells were shifted to 32°C for 0, 10 or 20 minutes as indicated, fixed and visualized for GFP fluorescence by confocal microscopy. (B) Transfected cells were infected at an MOI of 30 PFU/cell, incubated at 40°C for 3 hours and shifted to 32°C for 0, 10 minutes or 20 minutes as indicated, fixed and visualized for GFP fluorescence by confocal microscopy. For each panel, an image was selected to represent most abundant class of expression pattern for that condition and time point. Arrows identify VSVG-ts045-GFP puncta and arrowheads identify Golgi-like patterns. (C) The numbers of cells with ER-like, ER with puncta, and Golgi-like patterns were determined for both infected and uninfected cells at 0, 5, 10 and 20 minutes after temperature shift. Three cover slips per time point were evaluated and the percentage of cells with each pattern category was determined. At least 50 cells per coverslip were evaluated. For each type of pattern, the percentage of cells is plotted as a function of time for uninfected (■) and infected (□) cells.

Poliovirus infection induces dispersion of the Golgi network into distinct membranous compartments

In principle, the ERGIC-to-Golgi block could be the direct result of the dispersion of the Golgi known to occur during poliovirus infection, if, for example, cargo leaving the ERGIC cannot progress through the secretory pathway because the Golgi has been dispersed (Egger et al., 1999; Egger et al., 2000). To characterize the dynamics of poliovirus-induced Golgi disruption further, we used time-lapsed video microscopy of COS-7 cells that expressed a GFP-tagged transmembrane Golgi protein, galactosyl transferase (GT-GFP). As previously described, uninfected cells showed a dynamic Golgi complex, with tubules and vesicles emanating and returning to the structure (Fig. 5; supplementary material Movies 1-4) (Sciaky et al., 1997). Despite its dynamic nature, however, the Golgi organelle remained as one cohesive structure in the juxtanuclear region of the cell (Fig. 5A-C;

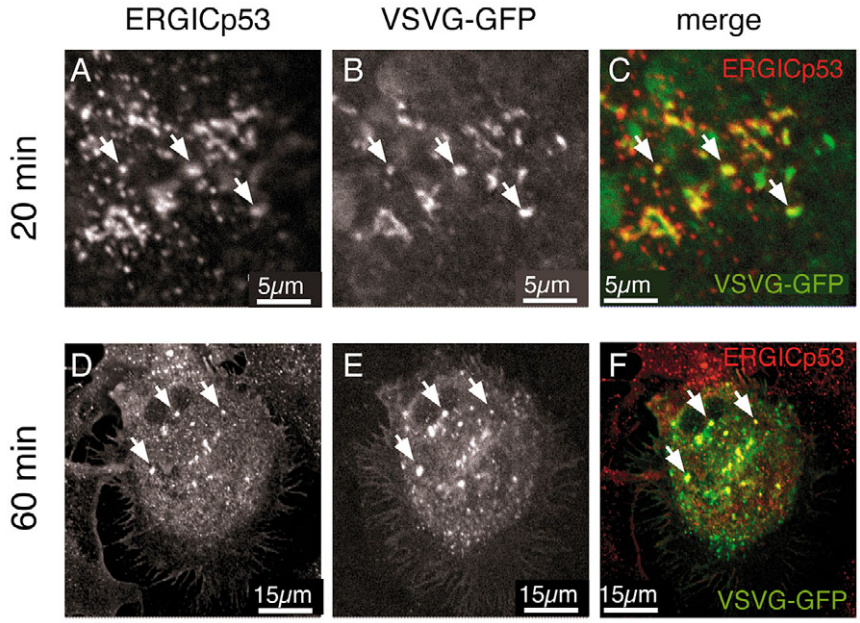

Fig. 3. Colocalization of punctate VSVG-ts045-GFP staining with ERGIC p53. (A-F) Huh7 cells were transfected with VSVG-ts045-GFP-expressing plasmid and infected with poliovirus as in Fig. 2. After 3 hours of infection at 40°C, the cells were shifted to 32°C and incubation continued for either 20 minutes (A-C) or 60 minutes (D-F). After fixation, cells were labeled with an anti-ERGIC p53 antibody and visualized by confocal microscopy for indirect immunofluorescence of ERGICp53 (A,D) and GFP fluorescence (B,E). (C,F) Merged images.

supplementary material Movie 1). In poliovirus-infected cells, the Golgi complex resembled that of uninfected cells up to 1 hour post infection. Between 60 and 90 minutes after infection, however, the Golgi appeared to disperse into many dynamic vesicles and tubules of heterogeneous size (Fig. 5D-F; supplementary material Movie 2). These Golgi-derived structures moved rapidly throughout the cell but did not return to form a cohesive juxtanuclear Golgi structure. Notably, as infection progressed, GT-GFP fluorescence became diffuse, suggesting a further fragmentation of the Golgi vesicles and tubules.

The diffuse appearance of the Golgi complex during poliovirus infection could arise either from its fragmentation

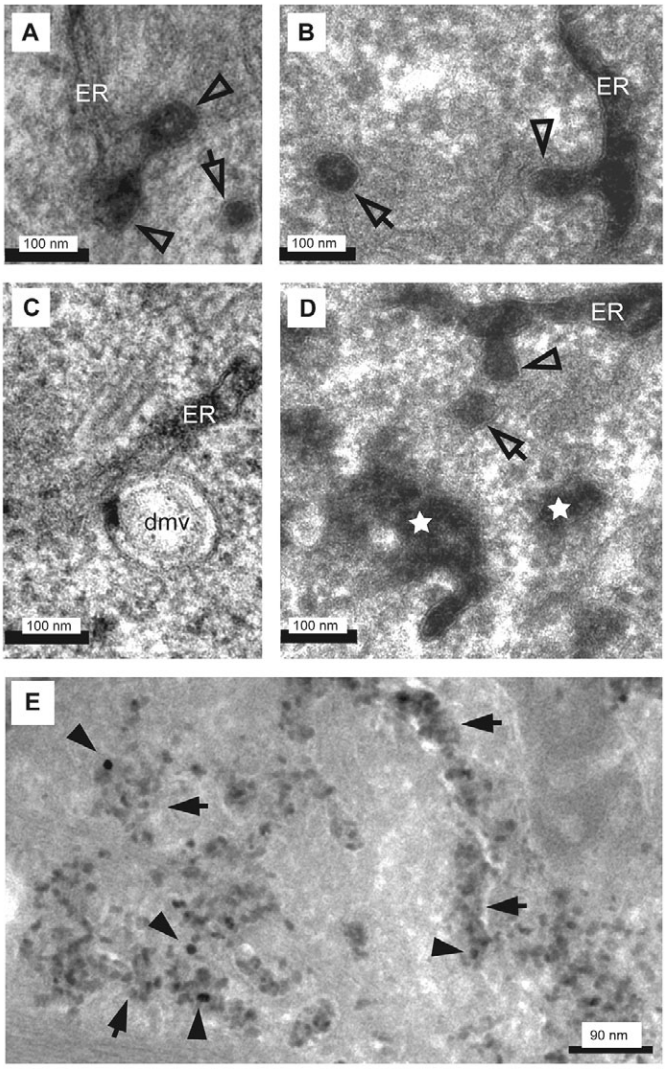

Fig. 4. EM of accumulated secreted alkaline phosphatase (SEAP) activity in uninfected and poliovirus-infected cells. (A-E) Huh7 cells were transiently transfected with SEAP-expressing plasmid pGeneGrip™ for 16 hours and either (A) mock-infected or (B-E) infected with poliovirus for 4 hours at an MOI of 30 PFU/cell. Cells were fixed and incubated with a solution containing glycerol phosphate and lead citrate, so that alkaline phosphatase activity would lead to the formation of electron-dense lead citrate. Samples were either processed for (A-D) conventional embedding in epoxyresin or (E) cryosectioning. Thawed cryosections were immunogold-labelled with an affinity-purified polyclonal rabbit anti-ERGICp53 antibody followed by a 15-nm gold-conjugated protein-A incubation. Ultrathin sections (~60-80 nm) of all samples were analyzed by EM. Low magnification confirmed that cells shown in B-E were infected, as evidenced by condensed nuclear morphology and the presence of numerous virus-induced vesicular structures (data not shown). Empty arrowheads mark budding structures at ER membranes filled with electron-dense precipitate. Empty arrows identify small (~80 nm) vesicles filled with precipitate. Stars mark precipitate-filled tubular-vesicular structures. (E) Solid arrowheads identify 15-nm gold particles; solid arrows identify precipitate-filled tubular-vesicular structures. ER, structures morphologically consistent with endoplasmic reticulum; dmv, double-membraned vesicle.

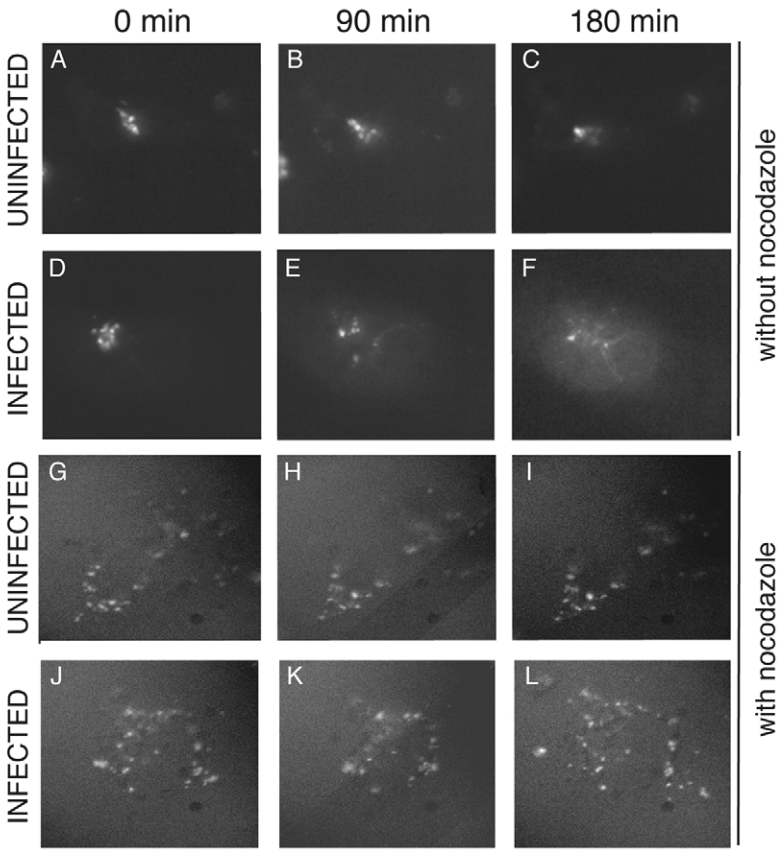

Fig. 5. Dynamics of the Golgi complex in poliovirus-infected cells. COS-7 cells were transfected with plasmid (GT-GFP) that expressed Golgi resident protein galactosyl transferase fused to GFP and incubated for 16 hours at 37°C. Before mock infection (A,C) or infection with poliovirus at an MOI of 10 PFU/cell (B,D), cells were pretreated for 1.5 hours in medium alone or in medium containing 5 μg/ml nocodazole as indicated. Cells were placed on a heated 37°C stage and images were obtained by fluorescence microscopy every 1.5 minutes for up to 5 hours, the images shown were taken 90 minutes apart. A complete set of images is provided as supplementary material Movies 1-4.

into minute vesicles or from its redistribution into the ER, as is observed upon brefeldin A (BFA) treatment (Lippincott-Schwartz et al., 1989). To test explicitly whether the Golgi redistributes into the ER during infection, we employed an endoglycosidase H (Endo H) assay. ER-specific glycosylation can be removed by Endo H digestion, whereas the acquisition of Golgi-specific modifications renders the glycoproteins resistant to Endo H. It has been shown previously (Doedens and Kirkegaard, 1995) that, VSVG that is newly synthesized during poliovirus infection remains primarily in an Endo-H-sensitive form, acquiring Endo H resistance at a rate three to five times slower than in uninfected cells, consistent with the inhibition of ER-to-Golgi traffic by poliovirus somewhere between the ER and the medial Golgi. As expected, at 40°C, VSVG-ts045-GFP remained Endo-H-sensitive (Fig. 6A, lanes 1 and 2). Upon shift to 32°C, VSVG-ts045-GFP acquired Endo H resistance, indicating that it was trafficked to the Golgi complex (Fig. 6A, lanes 3 and 4). In the presence of BFA, the VSVG-ts045-GFP protein acquired Endo H resistance without temperature shift (Fig. 6A, lanes 5 and 6), due to the known redistribution of Golgi enzymes into the ER upon BFA treatment (Lippincott-Schwartz et al., 1989). By contrast, in poliovirus-infected cells, VSVG-ts045-GFP retained the Endo H sensitivity characteristic of pre-Golgi structures at 40°C (Fig. 6A, lanes 7 and 8). This indicates that the diffuse Golgi membranes observed in infected cells do not redistribute into the ER as a result of poliovirus infection.

We next determined whether the diffuse Golgi staining observed in poliovirus-infected cells (Fig. 5F) represented small, fragmented Golgi vesicles or the complete disintegration of the Golgi complex, with its contents released into the cytoplasm. Sucrose flotation gradients were used to separate membranous and cytoplasmic components according to their

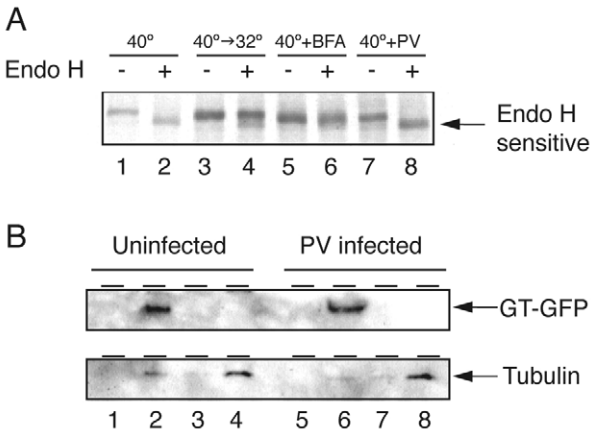

Fig. 6. Characteristics of Golgi dispersion during poliovirus infection. (A) Golgi-specific glycosylation of VSVG-ts045-GFP was monitored under various conditions. COS-7 cells were transfected with plasmid that expressed VSVG-ts045-GFP, incubated overnight at 40°C, pulse-labeled with [^{35}S]-methionine, and incubated with unlabeled methionine under the conditions described below. Cells were either mock-infected and kept at 40°C (lanes 1 and 2), shifted to 32°C for 30 minutes (lanes 3 and 4), treated with 2 μg/ml BFA for 1 hour at 40°C (lanes 5 and 6) or infected with poliovirus at 40°C for 4 hours (lanes 7 and 8). Labeled VSVG-ts045 was immunoprecipitated from cell extracts and digested with Endo H or not as indicated. Protein samples were analyzed by SDS-PAGE and visualized by autoradiography. Arrow indicates Endo-H-sensitive VSVG-ts045-GFP. (B) Membrane association of Golgi marker galactosyl transferase fused to GFP (GT-GFP) in uninfected and poliovirus-infected cells. COS-7 cells were transfected with plasmid that expressed GT-GFP and then either mock-infected or infected with poliovirus at an MOI of 10 PFU/ml for 3.5 hours. Whole-cell extracts were brought to 59% sucrose, overlaid with one 2-ml layer of 52% sucrose and a second 2-ml layer of 29% sucrose and centrifuged for 90 minutes at 196,000 ***g*** in an SW41 rotor. Fractions were collected and subjected to TCA precipitation. Proteins were displayed by SDS-PAGE, and the GT-GFP protein visualized by immunoblot. Fractions that contained 29% sucrose (lanes 1, 5), the 29%/52% interface (2, 6), 52% sucrose (lanes 3, 7) and 59% sucrose (lanes 4, 8) are shown.

characteristic specific density coefficients. Membranous vesicles are known to fractionate at the 29-52% interface, whereas soluble proteins and protein aggregates remain in the dense 59% sucrose layer. In uninfected cells, GT-GFP concentrated in the interface between the 29% and 52% sucrose layer as expected; whereas tubulin, known to be cytosolic, was predominately found in the 59% sucrose layer (Fig. 6B). This pattern did not change in poliovirus-infected cells, indicating that GT-GFP remained associated with intracellular membranes, presumably in small vesicles. It is important to note that under our experimental conditions we tracked the entire cellular population of GT-GFP and not only newly synthesized protein. Therefore, this experiment was designed to follow the proteins present in the Golgi complex at steady-state before infection occurred.

Distinct modes of poliovirus-induced and nocodazole-induced disruption of the Golgi network

Because microtubules participate in maintaining Golgi structure and microtubule depolymerization is known to result in the reorganization of the Golgi complex, we next investigated the role of microtubules in the poliovirus-induced Golgi dispersion. In uninfected cells, depolymerization of microtubules by nocodazole treatment resulted in the reorganization of the Golgi complex into characteristic mini-stacks, which appeared as punctuate structures throughout the cell [Fig. 5G-H; supplementary material Movie 3; (Thyberg and Moskalewski, 1985)]. These nocodazole-induced mini-stacks were clearly different from and larger than the dispersed Golgi-derived structures observed during poliovirus infection (Fig. 5F). We then examined whether poliovirus infection further affected nocodazole-induced mini-stacks to yield the diffuse fragmented staining observed in untreated infected cells (Fig. 5F). Notably, when nocodazole-treated cells were infected with poliovirus, the complete dispersion observed in untreated, infected cells was not observed (Fig. 5J-L, compare Fig. 5I with 5L; supplementary material Movie 4). Therefore, nocodazole blocks the morphological changes leading to minute Golgi vesicles in poliovirus-infected cells.

To analyze further the nocodazole-induced Golgi mini-stacks formed in infected and uninfected cells, we employed confocal microscopy using two different markers for the Golgi complex, GM130 and β-COP. GM130 is a resident Golgi protein and β-COP, a component of COPI vesicles, is present at steady-state at higher concentrations on cis-Golgi membranes. The half-life of GM130 is longer than the time course of poliovirus infection; therefore, the GM130 immunofluorescence signal study here is likely to reflect the localization of the resident Golgi marker before poliovirus infection. β-COP, on the other hand, cycles on and off the Golgi complex and COPI vesicles from the cytosol. As shown in Fig. 7, both GM130 and β-COP dispersed into very small punctate structures during poliovirus infection, with GM130 fluorescence showing a discrete punctuate pattern and β-COP presenting a more diffuse arrangement (compare Fig. 7C with 7G). However, in the presence of nocodazole, both markers colocalized to larger puncta whose morphology was not greatly altered by poliovirus infection (compare Fig. 7B with 7D, and 7F with 7H). Furthermore, we examined the distribution of poliovirus 2C protein, a marker for the virus replication complex. We found that, at least at this resolution, nocodazole modified the pattern of 2C staining only by making it juxtanuclear and more disperse throughout the cytoplasm (see supplementary material Fig. S2). Thus, whereas poliovirus replication has been previously shown to be insensitive to nocodazol treatment (Doedens et al., 1994), the more complete Golgi fragmentation induced by poliovirus – as judged by both GM130 and β-COP markers – was prevented by pre-treatment with nocodazole and, thus, must require intact microtubules.

When visualized by EM, the nocodazole-induced structures from infected and uninfected cells were comparable in size and morphology, containing both stacked Golgi membranes and

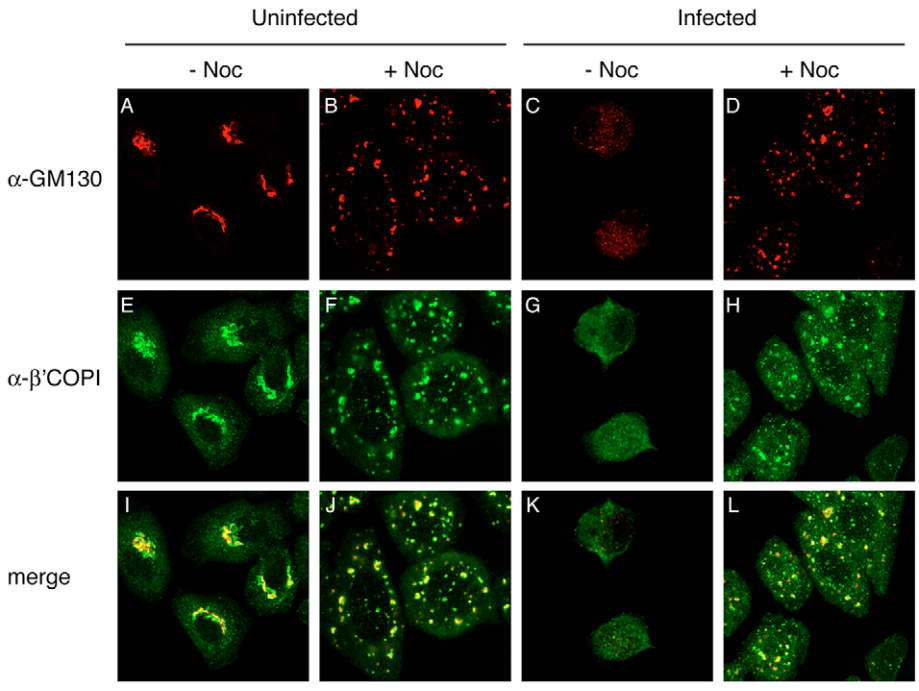

Fig. 7. Effect of nocodazole treatment on Golgi dispersion in poliovirus-infected cells. The localization of two different Golgi markers, GM130 and β-COP, were monitored by confocal immunofluorescence microscopy. (A-L) HeLa cells were pretreated with 10 μg/ml nocodazole (+Noc) or with medium without nocodazole (–Noc) for 1.5 hours Cells were then mock-infected (uninfected) or infected with poliovirus (MOI=10 PFU/ml) in the presence or absence of 10 μg/ml nocodazole. Cells were fixed at 3.5 hours post infection. Cells grown on cover slips were processed for indirect immunofluorescence and confocal microscopy as shown; the other cells in the dish were processed for conventional EM (see Fig. 8). The Golgi complex was stained with a murine monoclonal antibody directed against GM130 (red; A-D) and an affinity-purified polyconal rabbit antibody against β-COP (green, E-H) that detects COPI present on Golgi, ERGIC and COPI vesicular structures.

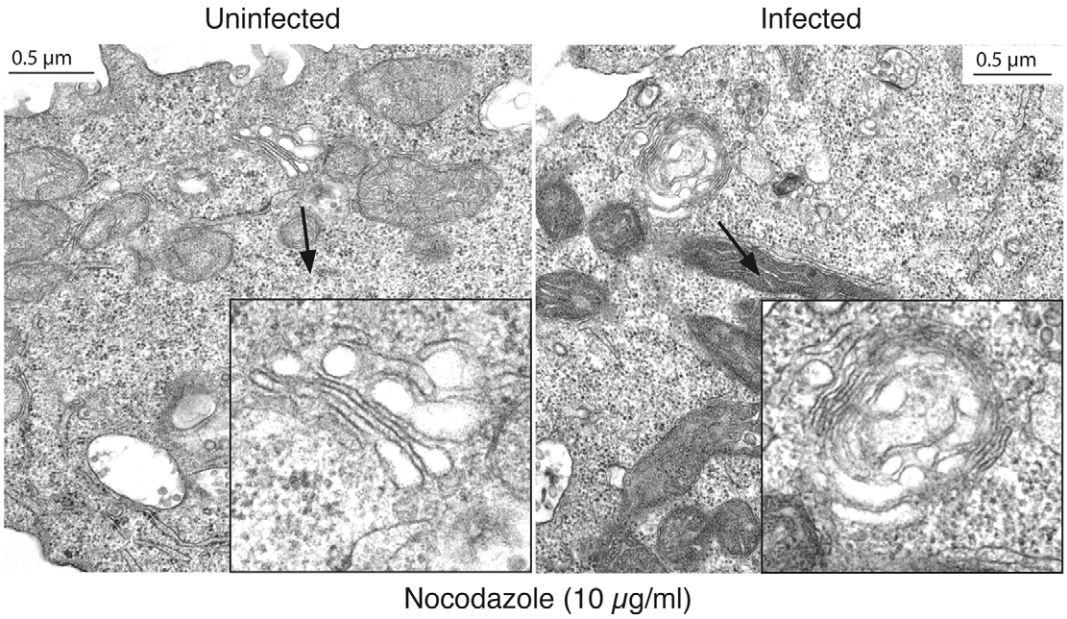

Fig. 8. Ultrastructure of a Golgi complex following nocodazole treatment of uninfected and poliovirus-infected cells. Cells from the experiment shown in Fig. 7 were processed for EM and ultrathin sections (60 nm) were analyzed. For both uninfected and infected cells, the arrows connect representative Golgi mini-stacks at low and high (inset) magnifications.

associated dilated vesicles (Fig. 8 and supplementary material Fig. S1). In uninfected cells, these structures were shown to be competent for protein secretion (Fig. 9). The similar morphology of these Golgi mini-stacks in poliovirus-infected cells suggests that they would also be competent to accept protein traffic. Therefore, we consider it unlikely that the inhibition of ERGIC-to-Golgi traffic during poliovirus infection, which can occur in the presence of nocodazole, is caused by the dispersion of the Golgi complex. Instead, it is likely to be caused by another, upstream event, perhaps exerting a direct effect on ERGIC membranes.

A dispersed Golgi complex can support secretion in uninfected cells and in cells infected by 3A-2 poliovirus mutant, but not in poliovirus-infected cells

The finding that the nocodazole-induced mini-stacks were resistant to further disruption by poliovirus provided an opportunity to test whether the poliovirus block of secretion was due to the dispersion of the Golgi complex. First, we confirmed that dispersion of the Golgi complex by nocodazole during long incubation times does not in itself block protein secretion (Cole et al., 1996; Rogalski et al., 1984). Accordingly, we monitored the secretion of SEAP protein over time in the presence and absence of pre-treatment with nocodazole to depolymerize microtubules. In these experiments, SEAP was expressed under the control of the EMCV IRES to ensure its translation in both uninfected and infected cells. As described, anterograde protein secretion was not dependent on microtubule integrity (Fig. 9C) (Cole et al., 1996; Rogalski et al., 1984). By contrast, treatment with BFA, which causes the Golgi to reabsorb onto the ER, did inhibit SEAP secretion in this system (Fig. 9B). We then examined whether nocodazole pretreatment affected the block of secretion in poliovirus-infected cells. In the absence of nocodazole, SEAP secretion was inhibited at 3 hours post infection, although SEAP protein continued to be synthesized and to accumulate intracellularly (Fig. 9D). Pretreatment with nocodazole did not affect the poliovirus-induced inhibition of SEAP secretion (Fig. 9E). Thus, it is unlikely that inhibition of secretion by poliovirus infection is directly caused by Golgi dispersion.

To distinguish the inhibition of protein secretion and Golgi dispersion by a method that does not employ nocodazole treatment, we monitored Golgi dispersion and protein secretion in cells infected with a mutant poliovirus that is known to display reduced inhibition of protein secretion. The mutant virus, 3A-2, contains a single amino acid insertion in the 3A coding region (Bernstein et al., 1985). Mutant 3A-2 protein, when expressed in isolation, causes a reduced inhibition of ER-to-Golgi traffic compared with wild-type 3A protein (Doedens et al., 1997) and cells infected with 3A-2 mutant virus secrete much higher levels of several cytokines than wild-type-infected cells (Dodd et al., 2001).

Cells infected with 3A-2 mutant virus secreted more SEAP than wild-type infected cells, although secretion was still somewhat inhibited relative to uninfected cells (Fig. 10A). Fig. 10B shows the dispersion of two different Golgi markers: GM130, a resident protein of the trans-Golgi, and GalT-GFP, which localizes to the cis-Golgi. In cells infected with either wild-type or 3A-2 mutant poliovirus, these markers are dispersed both from their juxtanuclear location and from each other. No difference in the extent of Golgi fragmentation was observed in many comparisons of wild-type and 3A-2 infected cells (Fig. 10B and data not shown). We conclude, that Golgi fragmentation per se is not sufficient to block protein secretion in poliovirus-infected cells.

Discussion

During infection with poliovirus, the inhibition of host protein secretion is evident by 2 hours post infection (Doedens et al.,

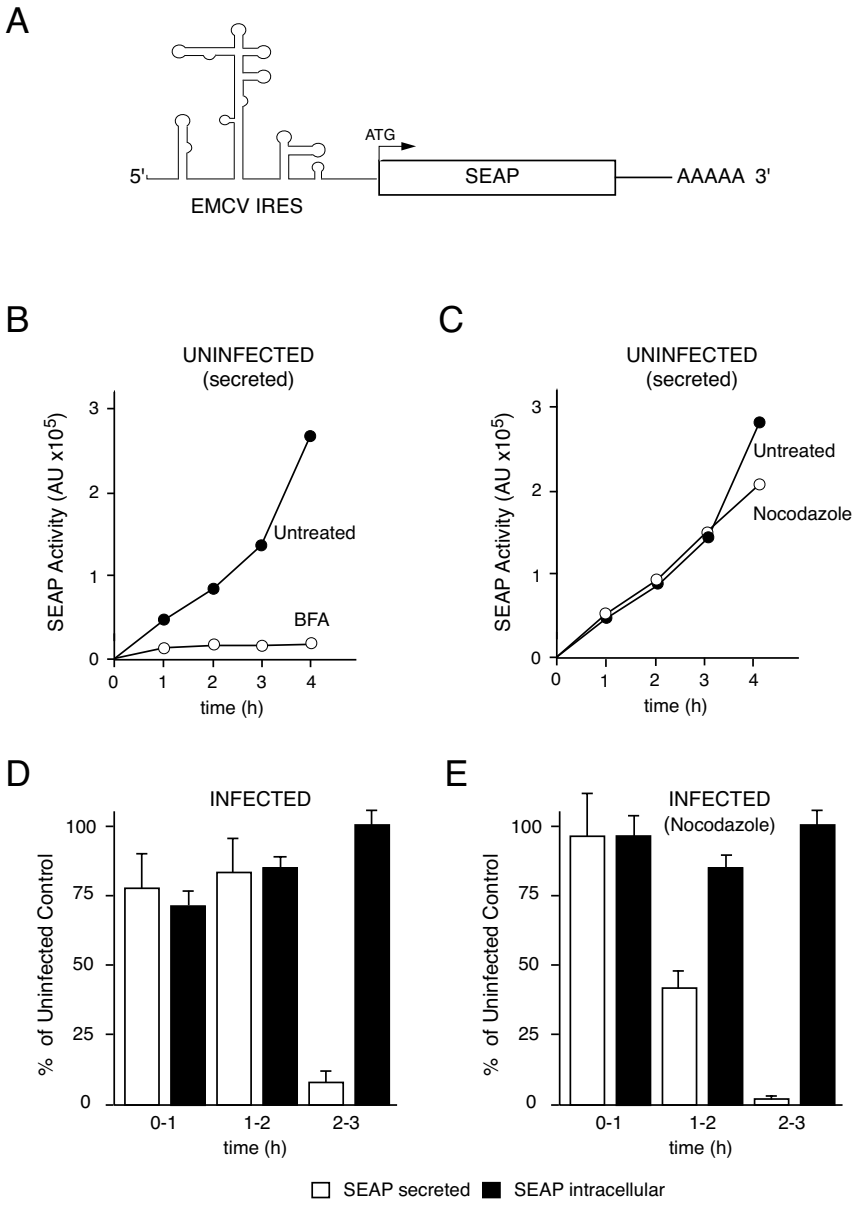

Fig. 9. Effect of nocodazole on SEAP secretion in uninfected and poliovirus-infected cells. COS-7 cells were transfected with a plasmid, pIRES-SEAP, that expressed (A) SEAP protein under the translational control of the IRES element from encephalomyocarditis virus (EMCV) to ensure effective translation in poliovirus-infected cells. (B) Transfected COS-7 cells were incubated for 16 hours at 37°C with or without 2 μg/ml BFA as indicated. Aliquots from the supernatants were sampled every hour from both cultures and assayed for SEAP activity. (C) Transfected COS-7 cells were either incubated with serum-free medium with or without 5 μg/ml nocodazole for 1.5 hours The medium was then replaced with fresh medium with or without nocodazole and aliquots taken every hour to determine SEAP activity. (D) Transfected COS-7 cells were mock-infected or infected with poliovirus at an MOI of 10 PFU/cell. SEAP activity was assayed in both the supernatants and the cells of mock-infected and infected cells at the time points indicated. The percentage of SEAP activity in infected cells compared with that in uninfected cells is plotted for secreted and intracellular SEAP as a function of time post infection. Experiments were performed in triplicate and the standard error is shown. (E) pIRES-SEAP-transfected cells were treated for 1.5 hours with serum-free medium with or without 5 μg/ml nocodazole and either mock-infected or infected with poliovirus at an MOI of 10 PFU/cell. Aliquots of medium were sampled every hour and assayed for SEAP activity. The percentage of extracellular and intracellular SEAP activity in infected cells compared with uninfected cells as a function of time after infection in the presence of nocodazole is shown.

1997; Doedens and Kirkegaard, 1995). Inhibiting secretion allows escape from immune surveillance by blocking a number of antiviral-associated responses, including cell-surface expression of MHC class I molecules (Deitz et al., 2000) and TNF receptors (Neznanov et al., 2001), secretion of interleukins 6 and 8 that help recruit lymphocytes, and secretion of type 1 interferon to induce antiviral states in infected cells (Dodd et al., 2001). The decreased rate of acquisition of trans-Golgi-specific modifications that accompany normal ER-to-Golgi traffic observed during poliovirus infection indicated that the block in secretion was somewhere between the ER and the medial Golgi. However, the specific mechanistic step at which ER-to-Golgi traffic is blocked had not been determined. Here, we employed a temperature-sensitive allele of VSVG, expressed as a fusion protein with GFP, to determine the precise step blocked by poliovirus infection. Our basic strategy was to accumulate the cargo VSVG-ts045-GFP in the ER prior to poliovirus infection by incubation at 40°C. Upon poliovirus infection, cells were downshifted to the permissive temperature to follow the progress of the cargo through the secretory pathway. Instead of trafficking to the Golgi, poliovirus infection caused VSVG-ts045-GFP to remain in ER-like membranes and to colocalize in punctate structures with markers of the ER-to-Golgi intermediate compartment (ERGIC) (Figs 1-4). The rate of formation of ERGIC membranes that contained VSVG-ts045 cargo was unchanged between infected and uninfected cells (Fig. 2). Furthermore, numerous 80-nm vesicles filled with secretory cargo were observed in poliovirus-infected, as well as in uninfected, cells (Fig. 4). Therefore, we conclude that poliovirus infection inhibits secretion by blocking traffic between the intermediate compartment and the Golgi. It is possible that additional steps are blocked as well, but this is the first stage at which the protein secretion complex inhibited during poliovirus infection.

What might be the mechanism by which traffic from the

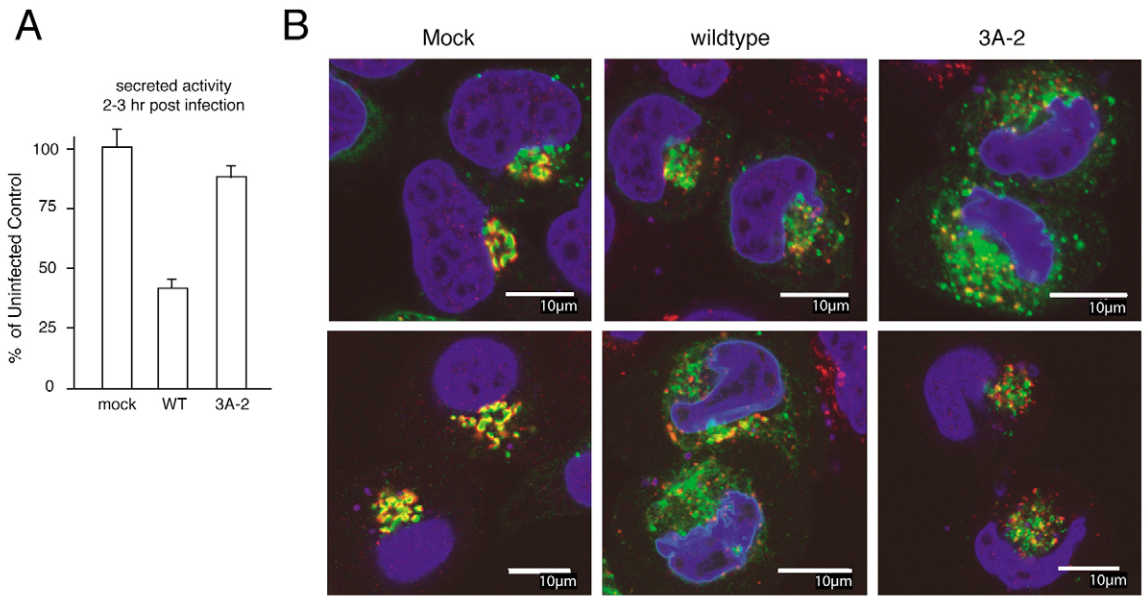

Fig. 10. Dispersed of the Golgi complex in cells infected with 3A-2 poliovirus secretion mutant. (A) COS-7 cells were transfected as in the experiment of Fig. 9 with pIRES-SEAP. Transfected COS-7 cells were mock-infected or infected with wild-type (WT) or mutant 3A-2 (3A-2) poliovirus at an MOI of 10 PFU/cell. SEAP activity was assayed in the cell culture supernatants. (B) COS-7 cells were transfected with plasmid (GT-GFP) that expressed Golgi resident protein galactosyl transferase fused to GFP and incubated for 16 hours at 37°C. Cells were mock-infected or infected with wild-type or mutant 3A-2 poliovirus at an MOI of 10 PFU/cell. Cells were incubated for 3 hours at 37°C, fixed and visualized for GFP fluorescence (green) and immunoflurescence using a anti GM130 antibody (red) by confocal microscopy.

ERGIC is inhibited? In principle, this might result from the dispersion of the Golgi known to occur during poliovirus infection, as this could prevent the ERGIC-derived vesicles from docking on the Golgi. However, our results do not support this hypothesis. Golgi dispersion can be prevented by nocodazole treatment, which leads to the formation of transport-competent Golgi mini-stacks (Figs 8, 9). Importantly, nocodazole treatment does not itself inhibit anterograde traffic (Fig. 5), indicating that the Golgi mini-stacks themselves are competent for transport. However, even when these Golgi structures were preserved in infected cells, ER-to-Golgi transport was inhibited. Furthermore, Golgi dispersion was found to be similar in cells infected with wild-type virus and with a mutant virus that was much less effective in inhibiting protein secretion (Fig. 10). These results argue that poliovirus inhibits protein secretion by targeting components of the ER-to-Golgi intermediate compartment membranes rather than by inducing Golgi dispersion.

Viral protein 3A has been shown to block ER-to-Golgi traffic on its own (Doedens and Kirkegaard, 1995) at the ERGIC-to-Golgi step (Wessels et al., 2005). This activity correlated with direct interactions with cellular proteins Lis1 (Kondratova et al., 2005) and GBF1 (Wessels et al., 2006). Notably, overexpression of cellular protein Arf1 or GBF1 abrogates the inhibition by coxsackie virus 3A of ER-to-Golgi traffic (Wessels et al., 2006). Given that Arf1 and GBF1 appear to be required for transport from the ERGIC to Golgi, all these data are consistent with a model in which 3A specifically inhibits the function of GBF1 by interacting with its N-terminus (Wessels et al., 2006). However, loss-of-function phenotypes for Lis1 and GBF1 have not been reported in the context of 3A protein expression or viral infection. Analysis of the effects of individual viral proteins may facilitate understanding the effects of viral infection, although their combined action during infection may not be successfully mimicked. Further investigation will be required to link our findings that poliovirus infection blocks the ERGIC-to-Golgi step with the effects observed upon ectopic expression of various viral proteins that affect protein secretion (Barco and Carrasco, 1995; Cho et al., 1994; Doedens et al., 1997; Doedens and Kirkegaard, 1995; Sandoval and Carrasco, 1997).

Although it has been suggested that redirection of Arf1 and β-COP cause the inhibition of ER-to-Golgi traffic (Belov and Ehrenfeld, 2007), it is noteworthy that β-COP, a component of the COP1 coat, remained Golgi-associated during poliovirus infection of nocodazole-treated cells (Fig. 8). Under these conditions, ER-to-Golgi traffic was still inhibited (Fig. 5). Therefore, the dissociation of COP1 proteins from the Golgi is not likely to cause the inhibition of protein secretion, because this block was still observed in the presence of nocodazole (Fig. 5). We conclude that the mechanism for inhibition of ERGIC-to-Golgi traffic during poliovirus infection is not the release of COP1 proteins from the Golgi or the dispersion of the Golgi, but perhaps a specific effect on the ERGIC itself. Indeed, this effect could be mediated by the inhibition of GBF1 activation of Arf1 at ERGIC membranes by 3A (Wessels et al., 2006).

During poliovirus infection, three distinct, functionally separable effects on host-cell membranes occur. First, disassembly or vesiculation of the Golgi complex occurs during viral infection. This disassembly has been reported to occur following expression of viral 2B protein in isolation (Sandoval and Carrasco, 1997). However, vesiculation of the Golgi complex is not required for viral replication in tissue-

culture cells, as the intracellular yield of poliovirus is not altered during nocodazole treatment (Doedens et al., 1994). Second, all positive-stranded RNA viruses, including poliovirus, assemble their RNA replication complexes on intracellular membranes. For poliovirus, these membranes are 200-400 nm in diameter (cf. Fig. 4C). Their formation is independent of the ability of the virus to inhibit host protein secretion, because mutant viruses that do not inhibit protein secretion can display wild-type amounts of RNA replication and induce the formation of similar membranous vesicles (Dodd et al., 2001). Finally, poliovirus inhibits ERGIC-to-Golgi traffic. This effect is dispensable for virus replication in tissue-culture cells, but is likely to play a role during viral infection in animals. Further elucidation of the mechanisms by which viral proteins subvert cellular membrane systems will provide insight both into immune evasion by the virus and into the cell biology of protein traffic in mammalian cells.

Materials and Methods

Cells, plasmids and antibodies

The virus used was poliovirus, Mahoney serotype 1, derived from an infectious cDNA (Racaniello and Baltimore, 1981). COS-7, Huh7 and HeLa cells were grown in Dulbecco's modified Eagle's medium (DMEM)-F12 with 10% serum from newborn calfs and 100 units/ml of both penicillin and streptomycin at 37°C. Green fluorescent protein (GFP) fusion reporter constructs that expressed vesicular stomatitis virus G ts045 protein (VSVG-ts045-GFP), and galactosyl transferase (GT-GFP) were gifts of Jennifer Lippincott-Schwartz (NIH, Bethesda, MA) and Richard Scheller (Genentech). The SEAP expression vector (pGeneGrip™ Rhodamine/SEAP) was purchased from Gene Therapy Systems Inc. (San Diego, CA). The pIRES-SEAP expression vector was constructed by amplifying the SEAP gene by PCR from a pCMV-SEAP plasmid (Applied Biosystems, Foster City, CA) and cloned into the pIRES vector (Clontech, Mountain View, CA). Anti-2C C-terminus polyclonal antibodies were obtained by inoculation of the 2C C-terminal peptide (CNIGNCMEALFQ) into rabbits (HTI Bio-products, Ramona, CA). The ERGIC-53 monoclonal antibody was kindly provided by Hans-Peter Hauri (Biozentrum, Basel, Switzerland), the affinity-purified polyclonal rabbit antibody against ERGIC-p53/p58 was purchased from Sigma (St Louis, MO). Polyclonal rabbit antiserum directed against β-COP was kindly provided by J. Simpson (EMBL, Heidelberg, Germany). GM130 antibody was purchased from Transduction Laboratories (Greenland, NH), anti-GFP antibody used for immunoprecipitation was a kind gift from the laboratory of D. S. Bredt (UCSF, San Francisco, CA), and the anti-GFP antibody used for immunoblot was purchased from Clontech. Protein A conjugated with 15-nm gold was purchased from the University of Utrecht (The Netherlands).

Transfections and infections

COS-7 cells were transfected with Lipofectamine Plus (Invitrogen, Carlsbad, CA) and Huh7 cells were transfected with FuGene 6 (Roche Diagnostics, Basel, Switzerland) transfection reagents according to the manufacturer's recommendations. In most experiments, HeLa, Huh7 or COS-7 cells were infected with poliovirus Mahoney type 1 at the appropriate multiplicity of infection (MOI) for 15 minutes at room temperature, and the infection was allowed to proceed at 37°C. For experiments that required incubation at 40°C, pre-warmed PBS and medium was employed at each step. Briefly, cells were washed with PBS, virus was adsorbed for 15 minutes at 40°C, infected cells were washed one time with PBS and then medium was added. COS-7 or HeLa cells infected in the presence of nocodazole were first pre-treated for 1.5 hours at 37°C with medium containing 5 μg/ml or 10 μg/ml nocodazole virus was diluted with nocodazole-containing medium, added to the cells, incubated at room temperature for 15 minutes, then washed with nocodazole-containing medium. Fresh pre-warmed 37°C medium with nocodazole was then added and the infection proceeded at 37°C.

Temperature shifts

Temperature shifts from 40°C directly to 32°C were performed by removing the 40°C medium and replacing it with medium at 32°C. Temperature shifts in the presence of nocodazole were performed by replacing the 40°C medium with iced medium containing 5 μg/ml nocodazole and cells were subsequently incubated on ice for 10 minutes. The cold medium was aspirated and replaced with pre-warmed 32°C medium containing 5 μg/ml nocodazole and placed at 32°C. Mutant 3A-2 virus was derived as described previously (Dodd et al., 2001).

Secreted alkaline phosphatase (SEAP) assay

Subconfluent COS-7 cells were transfected with the pIRES-SEAP expression vector, incubated for 6 hours at 37°C, trypsinized and split into 12-well dishes, and incubated overnight at 37°C. Cells in the 12-well dishes were then either mock-infected with serum-free medium (SFM) or infected with poliovirus diluted in SFM at an MOI of 10 PFU/cell. For experiments performed in the presence of nocodazole, cells were pre-treated for 1.5 hours with SFM that contained 5 μg/ml nocodazole (SFM+nocodazole). Then, cells were either mock-infected with SFM+nocodazole or infected with poliovirus diluted in SFM+nocodazole at an MOI of 10 PFU/cell. After 30 minutes incubation at room temperature, cells were washed with SFM, then 1.0 ml pre-warmed 37°C SFM (with or without nocodazole) was added. The cells were placed in a 37°C incubator, and 55 μl aliquots of the medium were taken every hour. The aliquots were centrifuged at 2500 ***g*** for 2 minutes to remove any cells. The SEAP activity was assayed using a chemiluminescence kit (Clontech).

Immunofluorescence and microscopy

Cells grown on coverslips were fixed for 15 minutes with cold 3.5% paraformaldehyde in PBS. Incubation with the primary antibody was carried out in 2% serum from newborn calfs in PBS + 0.1% Triton X-100 (PBST) solution for 1 hour. The cells were then washed three times with PBST and subsequently incubated for 30 minutes with the secondary antibody in PBST. After three PBST washes, the slides were mounted with Vectashield (Vector Laboratories, Burlingame, CA). Standard epifluorescent microscopy was performed on a Leica DMLB microscope using a 40× lens (NA 0.75) and digital images were obtained using a CCD camera. Confocal microscopy of immunostained cells was performed with a Leica TCS^{SP2} confocal laser-scanning microscope. All images were imported to and processed in Adobe Photoshop and Adobe Illustrator. To obtain time-lapse microscopy, COS-7 cells were mock-infected or infected with poliovirus at an MOI of 10 PFU/cell, placed into a culture dish for live-cell microscopy (Bioptechs, Butler, PA) heated to 37°C. The chambers were placed on the stage at room temperature and either infected with poliovirus (MOI, 10) or mock-infected with PBS. After 15 minutes incubation at room temperature, pre-warmed 37°C medium was added, the heated stage set to 37°C, and images were taken every 1.5 minutes for up to 5 hours. Imaging was performed using a Zeiss Axiovert S100 TV inverted microscope equipped with a C-Apochromat (NA 1.2) 63× oil objective, a Hammamatsu 12-bit ORCA, interline CCD camera, a Sutter excitation and emission filter-wheel, and a Universal Imaging Corporation MetaMorph Imaging system. Individual images were compiled into a movie using Metamorph software.

[^{35}S]-methionine labeling and immunoprecipitations

COS-7 cells were transfected with VSVG-ts045-GFP and incubated at 40ºC overnight. The cells were then incubated for 1 hour in methionine- and serum-free medium, labeled with 100 μCi/ml [^{35}S]-methionine for 1 hour, then incubated with serum-containing medium and either shifted to 32°C, treated with 2 μg/ml brefeldin A (BFA) at 40°C, infected with poliovirus at an MOI of 10 PFU/cell at 40°C, or mock-infected and incubated at 40°C. The cells were scraped off in iced PBS, collected by centrifugation, and lysed in TEEN (25 mM Tris, 1 mM EDTA, 1 mM EGTA, 150 mM NaCl) with 0.2% SDS, for 10 minutes on ice. An equal volume of TEEN with 2% Triton X-100 was then added. The resulting extract was centrifuged at 14,000 ***g*** for 5 minutes and the supernatant stored at –20°C. Immunoprecipitations were preformed by incubating the extract with anti-GFP antibody for 1 hour at 4°C followed by 1-hour incubation with protein A sepharose (Sigma) at 4°C. The immunoprecipitate was washed 3 times for 10 minutes with TEEN + 1% Triton X-100 and then incubated with 50 μl Endo H buffer (150 mM β-mercaptoethanol, 50 mM sodium acetate, 0.3% SDS) at 100°C for 5 minutes to elute the proteins from the beads. One half of the sample was incubated with Endoglycosidase H (Boehringer Mannheim, Germany) and the other half with buffer alone at 37°C overnight. The samples were then separated on a 10% SDS PAGE, the gel dried, and then exposed to radiographic film.

Sucrose floatation gradients

COS-7 cells were transiently transfected with plasmid that expressed GT-GFP and either mock-infected or infected with poliovirus at an MOI of 10 PFU/cell. At 3.5 hours post infection, cells were removed from the plate by scraping in PBS, collected by centrifugation, resuspended in TEEN+10% glycerol, and lysed via 15 strokes in a 25-gauge syringe. Unbroken cells and nuclei were removed by centrifugation and the supernatant was stored at –20°C. The nominally 59% sucrose layer was made by mixing 100 μl of extract with 1 ml of 59% sucrose in TEEN. This layer was overlaid with 2 ml of 52% sucrose in TEEN and 2 ml of 29% sucrose in TEEN. Centrifugation was for 90 minutes an SW41 rotor at 196,000 ***g***. Fractions of 300 μl were collected by puncturing the tubes at the specified locations (29%, 29/52% interface, 52/59% interface, 59%). The fractions were precipitated with 10% TCA, collected by centrifugation, displayed by SDS-PAGE in a 10% gel, and subjected to immunoblotting using an anti-GFP antibody. The anti-GFP signal was removed by incubation of the nitrocellulose in stripping buffer [100 mM 2-mercaptoethanol, 2% SDS, 62.5 mM Tris-HCl (pH 6.7)] at 50°C for 30 minutes After two washes in TBST (a buffer containing 10 mM Tris-Borate, pH=7.5, 100 mM sodium chloride and 1% Triton X-100), the nitrocellulose was re-blocked and probed with an antibody directed against tubulin as described above.

Electron microscopy

For standard electron microscopy (EM), cells were fixed in 2% glutaraldehyde and 2% paraformaldehyde in 0.1 M cacodylate buffer (pH 7.2), and postfixed in 1% osmium tetroxide. The samples were then dehydrated in an ascending ethanol series and a final propylene oxide incubation and embedded in epoxy-resin EMbed-812 (Electron Microscopy Sciences, Hatfield, PA). After polymerization, ultrathin sections (60 nm) were cut on an Ultracut S ultramicrotome (Leica, Wetzlar, Germany), mounted on Formvar- and carbon-coated grids and counterstained with 1% aqueous uranyl acetate and 0.2% lead citrate. For cryo-immuno EM, samples were fixed in 0.2% glutaraldehyde and 2% paraformaldehyde in 0.1 M cacodylate buffer (pH 7.2), embedded in 10% gelatin and infiltrated with 2.3 M sucrose overnight. Sample blocks were mounted on cryoultramicrotomy pins and frozen in liquid nitrogen. Ultrathin sections (70 nm) were cut on an Ultracut cryoultramicrotome (Leica) at –125°C, picked up with a mixture (1:1) of 2% methylcellulose and 2.3 M sucrose and transferred to Formvar- and carbon-coated grids. For immunogold labeling, thawed cryosections were incubated in a blocking solution (PBS containing 1% BSA and 1% fish gelatin) for 10 minutes, then incubated with rabbit polyclonal antibody directed against ERGICp53 (Sigma) for 30 minutes, washed with blocking solution, and incubated with protein-A–gold (15 nm) for 30 minutes After a final washing step, sections were counterstained with 0.5% uranyl acetate in 2% methylcellulose and grids were dried.

To localize SEAP activity at the ultrastrucutural level, a histochemical method was employed (Mayahara et al., 1967; Yamamoto et al., 2003). Briefly, Huh7 cells were transiently transfected with a SEAP expression vector (pGeneGrip™, Gene Therapy Systems Inc.) for 16 hours and mock-infected or infected for 4 hours with poliovirus at an MOI of 30 PFU/cell. Cells were then chemically fixed either as for conventional embedding or cryo-sectioning as described above. After fixation, the samples were washed in 0.1 M cacodylate buffer (pH 7.2), then incubated for 60 minutes in a medium that contained 30 mM Tris-HCl (pH 8.5), 0.6% β-glycerolphosphate, 4 mM magnesium sulphate and 0.2% lead citrate (pH 10.0). Subsequently, cells were rinsed with distilled water and either processed for conventional embedding or cryosectioning as described above. The histochemical reaction allows the localization of SEAP activity by the formation of an electron-dense precipitate consisting of lead phosphate. Ultrathin sections (approx. 60-80 nm) of all samples were analyzed with a JEOL 1230 TEM at 80 kV and digital photographs were taken using a Gatan Multiscan 791 digital camera.

We are grateful to Judith Frydman, Amethyst Gillis and members of the Andino laboratory for their useful comments on the manuscript. We thank Hans-Peter Hauri, Jennifer Lippincott-Schwartz and David Bredt for generously sharing of reagents, and Alla El-Din El-Huuseini for technical help with the time-lapse microscopy. This work was supported by funds provided by the Public Health Service grant no. AI40085 to R.A. and a NSF pre-doctoral fellowship to O.B.

References

Balch, W. E., McCaffery, J. M., Plutner, H. and Farquhar, M. G. (1994). Vesicular stomatitis virus glycoprotein is sorted and concentrated during export from the endoplasmic reticulum. *Cell* **76**, 841-852.

Barco, A. and Carrasco, L. (1995). A human virus protein, poliovirus protein 2BC, induces membrane proliferation and blocks the exocytic pathway in the yeast Saccharomyces cerevisiae. *EMBO J.* **14**, 3349-3364.

Belov, G. and Ehrenfeld, E. (2007). Involvement of cellular membrane traffic proteins in poliovirus replication. *Cell Cycle* **6**, 36-38.

Bernstein, H. D., Sonenberg, N. and Baltimore, D. (1985). Poliovirus mutant that does not selectively inhibit host cell protein synthesis. *Mol. Cell. Biol.* **5**, 2913-2923.

Bienz, K., Egger, D. and Pasamontes, L. (1987). Association of polioviral proteins of the P2 genomic region with the viral replication complex and virus-induced membrane synthesis as visualized by electron microscopic immunocytochemistry and autoradiography. *Virology* **160**, 220-226.

Bienz, K., Egger, D., Pfister, T. and Troxler, M. (1992). Structural and functional characterization of the poliovirus replication complex. *J. Virol.* **66**, 2740-2747.

Caliguiri, L. A. and Tamm, I. (1970). The role of cytoplasmic membranes in poliovirus biosynthesis. *Virology* **42**, 100-111.

Cho, M. W., Teterina, N., Egger, D., Bienz, K. and Ehrenfeld, E. (1994). Membrane rearrangement and vesicle induction by recombinant poliovirus 2C and 2BC in human cells. *Virology* **202**, 129-145.

Clark, M. E., Lieberman, P. M., Berk, A. J. and Dasgupta, A. (1993). Direct cleavage of human TATA-binding protein by poliovirus protease 3C in vivo and in vitro. *Mol. Cell. Biol.* **13**, 1232-1237.

Cole, N. B., Sciaky, N., Marotta, A., Song, J. and Lippincott-Schwartz, J. (1996). Golgi dispersal during microtubule disruption: regeneration of Golgi stacks at perpherical endoplasmic reticulum exit sites. *Mol. Biol. Cell* **7**, 631-650.

Crawford, N., Fire, A., Samuels, M., Sharp, P. A. and Baltimore, D. (1981). Inhibition of transcription factor activity by poliovirus. *Cell* **27**, 555-561.

Dascher, C., Matteson, J. and Balch, W. E. (1994). Syntaxin 5 regulates endoplasmic reticulum to Golgi transport. *J. Biol. Chem.* **269**, 29363-29366.

Deitz, S. B., Dodd, D. A., Cooper, S., Parham, P. and Kirkegaard, K. (2000). MHC I-dependent antigen presentation is inhibited by poliovirus protein 3A. *Proc. Natl. Acad. Sci. USA* **97**, 13790-13795.

Dodd, D. A., Giddings, T. H., Jr and Kirkegaard, K. (2001). Poliovirus 3A protein limits interleukin-6 (IL-6), IL-8, and beta interferon secretion during viral infection. *J. Virol.* **75**, 8158-8165.

Doedens, J. R. and Kirkegaard, K. (1995). Inhibition of cellular protein secretion by poliovirus proteins 2B and 3A. *EMBO J.* **14**, 894-907.

Doedens, J., Maynell, L. A., Klymkowsky, M. W. and Kirkegaard, K. (1994). Secretory pathway function, but not cytoskeletal integrity, is required in poliovirus infection. *Arch. Virol. Suppl.* **9**, 159-172.

Doedens, J. R., Giddings, T. J. and Kirkegaard, K. (1997). Inhibition of endoplasmic reticulum-to-Golgi traffic by poliovirus protein 3A: genetic and ultrastructural analysis. *J. Virol.* **71**, 9054-9064.

Egger, D., Bolten, R., Rahner, C. and Bienz, K. (1999). Fluorochrome-labeled RNA as a sensitive, strand-specific probe for direct fluorescence in situ hybridization. *Histochem. Cell Biol.* **111**, 319-324.

Egger, D., Teterina, N., Ehrenfeld, E. and Bienz, K. (2000). Formation of the poliovirus replication complex requires coupled viral translation, vesicle production, and viral RNA synthesis. *J. Virol.* **74**, 6570-6580.

Ehrenfeld, E. (1982). Poliovirus-induced inhibition of host-cell protein synthesis. *Cell* **28**, 435-436.

Farabaugh, P. J. (1996). Programmed translational frameshifting. *Microbiol. Rev.* **60**, 103-134.

Flint, J. and Shenk, T. (1997). Viral transactivating proteins. *Annu. Rev. Genet.* **31**, 177-212.

Hauri, H. P., Kappeler, F., Andersson, H. and Appenzeller, C. (2000). ERGIC-53 and traffic in the secretory pathway. *J. Cell Sci.* **113**, 587-596.

Helentjaris, T. and Ehrenfeld, E. (1977). Inhibition of host cell protein synthesis by UV-inactivated poliovirus. *J. Virol.* **21**, 259-267.

Hirschberg, K. and Lippincott-Schwartz, J. (1999). Secretory pathway kinetics and in vivo analysis of protein traffic from the Golgi complex to the cell surface. *FASEB J.* **13** Suppl. 2, S251-S256.

Hirschberg, K., Miller, C. M., Ellenberg, J., Presley, J. F., Siggia, E. D., Phair, R. D. and Lippincott-Schwartz, J. (1998). Kinetic analysis of secretory protein traffic and characterization of golgi to plasma membrane transport intermediates in living cells. *J. Cell Biol.* **143**, 1485-1503.

Jackson, W. T., Giddings, T. H., Jr, Taylor, M. P., Mulinyawe, S., Rabinovitch, M., Kopito, R. R. and Kirkegaard, K. (2005). Subversion of cellular autophagosomal machinery by RNA viruses. *PLoS Biol.* **3**, e156.

Jen, G., Birge, C. H. and Thach, R. E. (1978). Comparison of initiation rates of encephalomyocarditis virus and host protein synthesis in infected cells. *J. Virol.* **27**, 640-647.

Jen, G., Detjen, B. M. and Thach, R. E. (1980). Shutoff of HeLa cell protein synthesis by encephalomyocarditis virus and poliovirus: a comparative study. *J. Virol.* **35**, 150-156.

Kliewer, S. and Dasgupta, A. (1988). An RNA polymerase II transcription factor inactivated in poliovirus-infected cells copurifies with transcription factor TFIID. *Mol. Cell. Biol.* **8**, 3175-3182.

Kondratova, A. A., Neznanov, N., Kondratov, R. V. and Gudkov, A. V. (2005). Poliovirus protein 3A binds and inactivates LIS1, causing block of membrane protein trafficking and deregulation of cell division. *Cell Cycle* **4**, 1403-1410.

Kuge, O., Dascher, C., Orci, L., Rowe, T., Amherdt, M., Plutner, H., Ravazzola, M., Tanigawa, G., Rothman, J. E. and Balch, W. E. (1994). Sar1 promotes vesicle budding from the endoplasmic reticulum but not Golgi compartments. *J. Cell Biol.* **125**, 51-65.

Lippincott-Schwartz, J., Yuan, L. C., Bonifacino, J. S. and Klausner, R. D. (1989). Rapid redistribution of Golgi proteins into the ER in cells treated with brefeldin A: evidence for membrane cycling from Golgi to ER. *Cell* **56**, 801-813.

Mayahara, H., Hirano, H., Saito, T. and Ogawa, K. (1967). The new lead citrate method for the ultracytochemical demonstration of activity of non-specific alkaline phosphatase (orthophosphoric monoester phosphohydrolase). *Histochemie* **11**, 88-96.

Messerschmitt, A. S., Dunant, N. and Ballmer-Hofer, K. (1997). DNA tumor viruses and Src family tyrosine kinases, an intimate relationship. *Virology* **227**, 271-280.

Moran, E. (1993). DNA tumor virus transforming proteins and the cell cycle. *Curr. Opin. Genet. Dev.* **3**, 63-70.

Moss, B., Ahn, B. Y., Amegadzie, B., Gershon, P. D. and Keck, J. G. (1991). Cytoplasmic transcription system encoded by vaccinia virus. *J. Biol. Chem.* **266**, 1355-1358.

Mountford, P. S. and Smith, A. G. (1995). Internal ribosome entry sites and dicistronic RNAs in mammalian transgenesis. *Trends Genet.* **11**, 179-184.

Nakielny, S. and Dreyfuss, G. (1999). Transport of proteins and RNAs in and out of the nucleus. *Cell* **99**, 677-690.

Neznanov, N., Kondratova, A., Chumakov, K. M., Angres, B., Zhumabayeva, B., Agol, V. I. and Gudkov, A. V. (2001). Poliovirus protein 3A inhibits tumor necrosis factor (TNF)-induced apoptosis by eliminating the TNF receptor from the cell surface. *J. Virol.* **75**, 10409-10420.

Nuoffer, C., Davidson, H. W., Matteson, J., Meinkoth, J. and Balch, W. E. (1994). A GDP-bound of rab1 inhibits protein export from the endoplasmic reticulum and transport between Golgi compartments. *J. Cell Biol.* **125**, 225-237.

Pind, S. N., Nuoffer, C., McCaffery, J. M., Plutner, H., Davidson, H. W., Farquhar, M. G. and Balch, W. E. (1994). Rab1 and Ca^{2+} are required for the fusion of carrier

vesicles mediating endoplasmic reticulum to Golgi transport. *J. Cell Biol.* **125**, 239-252.

Presley, J. F., Cole, N. B., Schroer, T. A., Hirschberg, K., Zaal, K. J. and Lippincott-Schwartz, J. (1997). ER-to-Golgi transport visualized in living cells. *Nature* **389**, 81-85.

Racaniello, V. R. and Baltimore, D. (1981). Cloned poliovirus complementary DNA is infectious in mammalian cells. *Science* **214**, 916-919.

Rogalski, A. A., Bergmann, J. E. and Singer, S. J. (1984). Effect of microtubule assembly status on the intracellular processing and surface expression of an integral protein of the plasma membrane. *J. Cell Biol.* **99**, 1101-1109.

Sandoval, I. V. and Carrasco, L. (1997). Poliovirus infection and expression of the poliovirus protein 2B provoke the disassembly of the Golgi complex, the organelle target for the antipoliovirus drug Ro-090179. *J. Virol.* **71**, 4679-4693.

Scales, S. J., Pepperkok, R. and Kreis, T. E. (1997). Visualization of ER-to-Golgi transport in living cells reveals a sequential mode of action for COPII and COPI. *Cell* **90**, 1137-1148.

Sciaky, N., Presley, J., Smith, C., Zaal, K. J., Cole, N., Moreira, J. E., Terasaki, M., Siggia, E. and Lippincott-Schwartz, J. (1997). Golgi tubule traffic and the effects of brefeldin A visualized in living cells. *J. Cell Biol.* **139**, 1137-1155.

Suhy, D. A., Giddings, T. H., Jr and Kirkegaard, K. (2000). Remodeling the endoplasmic reticulum by poliovirus infection and by individual viral proteins: an autophagy-like origin for virus-induced vesicles. *J. Virol.* **74**, 8953-8965.

Teterina, N. L., Gorbalenya, A. E., Egger, D., Bienz, K. and Ehrenfeld, E. (1997). Poliovirus 2C protein determinants of membrane binding and rearrangements in mammalian cells. *J. Virol.* **71**, 8962-8972.

Teterina, N. L., Gorbalenya, A. E., Egger, D., Bienz, K., Rinaudo, M. S. and Ehrenfeld, E. (2006). Testing the modularity of the N-terminal amphipathic helix conserved in picornavirus 2C proteins and hepatitis C NS5A protein. *Virology* **344**, 453-467.

Thyberg, J. and Moskalewski, S. (1985). Microtubules and the organization of the Golgi complex. *Exp. Cell Res.* **159**, 1-16.

Wessels, E., Duijsings, D., Notebaart, R. A., Melchers, W. J. and van Kuppeveld, F. J. (2005). A proline-rich region in the coxsackievirus 3A protein is required for the protein to inhibit endoplasmic reticulum-to-golgi transport. *J. Virol.* **79**, 5163-5173.

Wessels, E., Duijsings, D., Niu, T. K., Neumann, S., Oorschot, V. M., de Lange, F., Lanke, K. H., Klumperman, J., Henke, A., Jackson, C. L. et al. (2006). A viral protein that blocks Arf1-mediated COP-I assembly by inhibiting the guanine nucleotide exchange factor GBF1. *Dev. Cell* **11**, 191-201.

Yamamoto, K., Awogi, T., Okuyama, K. and Takahashi, N. (2003). Nuclear localization of alkaline phosphatase in cultured human cancer cells. *Med. Electron Microsc.* **36**, 47-51.

Yoneda, Y., Hieda, M., Nagoshi, E. and Miyamoto, Y. (1999). Nucleocytoplasmic protein transport and recycling of Ran. *Cell Struct. Funct.* **24**, 425-433.